Creep Behavior of Fine Grain, Low Carbon Allvac 718

C. N. Ruiz*, S. S. Mysore**, L. A. Jackman*, R. B. Lal**, A. A. Wereszczak***

* Teledyne Allvac, Research and Development
Monroe, North Carolina

**Alabama A&M University, Department of Physics
Normal, Alabama

*** Oak Ridge National Laboratory, High Temperature Materials Laboratory
Oak Ridge, Tennessee

Abstract

The aerospace materials community has demonstrated considerable interest in achieving improved properties in Alloy 718 by finer grain microstructures and better cleanliness. Its composition has been investigated in the past, in combination with standard and novel fine grain processing techniques, to improve low cycle fatigue capabilities. Lower carbon content is one compositional change that has been evaluated and debated for a number of years. Investigators are in agreement that tensile strength is not effected by low carbon, and that improved carbide distribution provides an opportunity for better fatigue properties. However, the effect on creep properties remains unresolved.

Production ingots of standard (0.025 wt% C) and low carbon (0.010 wt% C) Allvac 718 were processed to 5-inch diameter forged bar. Processing and heat treatment was aimed at producing fine grain microstructure and maximizing tensile properties. Two process techniques were used; 1) a fine grain process employing super and sub δ-solvus temperature forging, 2) a mini-grain process which involves an intentional δ-phase precipitation and sub δ-solvus forging. All material was direct age heat treated. Preliminary creep properties showed no difference between low carbon Allvac 718 and standard carbon Allvac 718. Supporting previous studies, the material displayed high tensile strength at room and elevated temperatures.

Creep and low cycle fatigue testing were not completed by the deadline for the written presentation. Copies of all creep and low cycle fatigue results will be available at the time of the oral presentation.

Superalloys 718, 625, 706 and Various Derivatives
Edited by E.A. Loria
The Minerals, Metals & Materials Society, 1994

Introduction

The materials community, aerospace in particular, has demonstrated considerable interest in increasing the fatigue capabilities of Alloy 718 through finer grain microstructures and improved material cleanliness. Responding to that interest, Teledyne Allvac has developed production conversion techniques to consistently produce fine grain Alloy 718 products. One technique involves controlled thermomechanical processing during press and rotary forging to produce fine grained material. Another process utilizes an intentional δ-phase precipitation to control grain growth during subsequent thermomechanical operations. Material cleanliness improvements have been achieved through electroslag remelting and melt control systems to minimize the occurrence of oxides and melt related defects.

Composition modifications to improve microcleanliness, however, have been slower to gain acceptance within the industry. Reducing the carbon content is one of those modifications that have been proposed and debated for a number of years. Distinct carbide distribution improvements, in the form of reduced stringer and cluster formation, occur when the carbon content is reduced to 0.010 wt% and below. As the grain size is reduced, carbide stringers and clusters become the predominant fatigue fracture initiation source in test specimens. Therefore, an improvement in low cycle fatigue properties is theoretically achievable if the maximum inherent flaw size can be reduced. However, no evaluations known to the authors have been publicly reported which supports or disproves this theory.

Another impedance to accepting lower carbon levels is conflicting reports on the effect of stress rupture properties. Several technical reports have been published with conflicting results since Stroup and Pugliese reported reduced stress rupture lives, low stress rupture ductility, and notch sensitivity when carbon was reduced below 0.057%.[1] Moyer reported no adverse effects on the stress rupture properties in heats of Alloy 718 with as little as 0.006 wt% C.[2] In addition, Jackman et. al. reported no adverse effects on either stress rupture or time to 0.2% creep between material with 0.008 wt% C and 0.027 wt% C.[3] In contrast, Banik et. al. reported reduced stress rupture properties in material with 0.006 wt% C compared to material from a heat with 0.033 wt% C.[4]

While stress rupture properties provide an indication of creep properties, wrought components do not typically fail in stress rupture. An investigation of the creep behavior would be more applicable, since turbine disks and shafts are designed to ensure blade retention and avoid growth, respectively. This report will provide preliminary results on whether creep properties of Alloy 718 are influenced by low carbon content.

Material Processing

Melting - Material for the program was processed from 20-inch diameter production ingots of low carbon and standard Allvac 718. The Nb content of the low carbon heat was reduced to account for a decrease in the amount of Nb partitioned to carbides. Both electrodes were subsequently electroslag remelted followed by vacuum arc remelting. Typical chemistries of the low carbon and standard carbon forged bar are shown in Table I.

Table I. Typical Composition of Low Carbon and Standard Carbon Forged Bar.

	Fe	Cr	Mo	Ti	Al	Nb+Ta	C	Ni
Low C	18.20	17.86	2.84	0.98	0.48	5.26	0.010	53.83
Std. C	17.91	17.93	2.89	0.97	0.47	5.38	0.025	53.52

Ingot Conversion - Two fine grain processing techniques were evaluated, namely fine grain and mini-grain processing. The fine grain process produces forged bar with maximum tensile properties and a fine grain microstructure. Mini-grain processing was investigated as a means of producing an ultra-fine grain microstructure in an attempt to optimize low cycle fatigue properties.

Press Forge Process - Following homogenization, ingot breakdown to rotary forge preform size was conducted at temperatures slightly above 2000°F with the final reductions at temperatures well above the δ-solvus. At this point the low carbon ingot was cut, permitting portions to be processed using different techniques. The standard carbon ingot remained whole.

Fine Grain Rotary Forge Process: To eliminate processing as a variable, the standard carbon ingot and a portion of the low carbon ingot were processed using a fine grain practice. The fine grain technique used was actually developed by Teledyne Allvac for high strength shafts applications.[5] However, the practice was similar to those used for producing forging billet. Initial rotary forging on a Model 55 GFM machine was conducted at temperatures slightly in excess of the δ-phase solvus temperature. At an intermediate size, the material was reheated at a temperature just below the δ-solvus and forged to the final size of approximately 5-inches in diameter.

Mini-grain Rotary Forge Process: Teledyne Allvac has developed standard mini-grain conversion practices based on the process developed by Brown, Boettner, and Ruckle.[6] A portion of the low carbon ingot was processed using a mini-grain practice aimed at reducing δ-phase, hence maximizing tensile strength. The rotary forge preform was given a shorter δ-phase heat treatment than the standard practice to precipitate just enough δ-phase to control grain growth. Initial rotary forging was conducted well below the δ-solvus to refine the grain size and spheroidize the δ-phase. The material was then reheated to a temperature close to the δ-solvus and forged to the final diameter of 5-inches.

Heat Treatment - All test material received a direct aged heat treatment as follows: 1350°F hold for 8 hours, furnace cool at 100°F per hour to 1150°F, hold for 8 hours, and air cool.

Experimental Procedure

The matrix of test conditions and quantities is shown in Table II. Material for mechanical property and metallographic specimens was cut from both ends of each bar. Representative photomicrographs were taken of the mid-radius location. Tensile and creep specimens were removed from the mid-radius location in the longitudinal orientation. Low cycle fatigue and stress rupture specimens were excised from the mid-radius location in the tangential orientation.

Not all creep or fatigue results were available at the deadline for the written presentation. Stress rupture conditions will be determined when more creep tests are completed. Copies of all creep, stress rupture, and low cycle fatigue results will be available at the time of the oral presentation.

Table II. Test matrix for mechanical testing.

Material, Process	Tensile: 75°F, 500°F, 1200°F	Creep: 1200°F/100 ksi	Creep: 1400°F/30 ksi	LCF: 300°F, A=1.0
Std. C, Fine Grain	4 ea.	6	6	12
Low C, Fine Grain	4 ea.	6	6	12
Low C, Mini-Grain	4 ea.	6	6	12

Creep Test Setup: The creep tests were conducted on commercial electromechanical tensile test machines at the High Temperature Materials Laboratory at Oak Ridge National Laboratory. The machines incorporate load displacement, and strain control capabilities (Model 1380 Low-cycle

Creep/Fatigue Machine, Instron Corp. Canton, MA). The desired control parameter-time profiles were controlled by trapezoidal function generators. The specimen grips, which were configured for buttonhead specimens (Figure 1), were located outside the compacted two zone resistance heat furnaces.

The grips were attached to the load frame using hydraulic couplers to minimize bending moments. Specimen displacements were measured over 25 mm gage length with direct contact extensometers employing remote capacitance sensors (Figure 2). By carefully controlling the temperature of both the measurement hardware and grip cooling water, resolutions of ≈0.5 μm could be achieved with these arrangements. Personal computers and data acquisition systems were used to monitor and store various output signals including displacement, load, load error, and test temperature. All creep tests were conducted in ambient air under electronic load control.

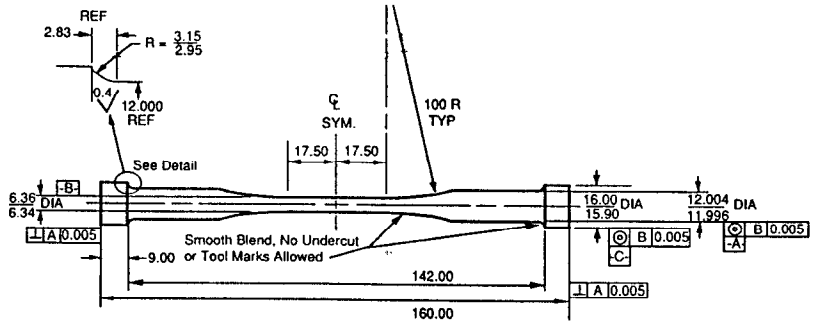

Figure 1. Creep test specimen. Dimensions in mm, xx dec. ±0.25.

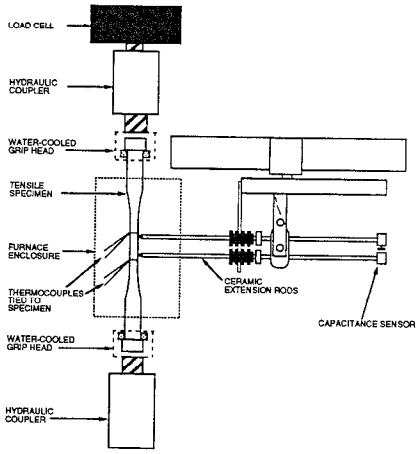

Figure 2. Schematic of loading configuration and equipment for creep tests.

Results and Discussion

Microstructure - The same microstructure response to fine grain processing was exhibited by the low carbon and standard carbon compositions The microstructure of the low carbon and standard carbon, fine grain processed material was uniform with an ASTM 8 grain size, as shown in Figure 3a and 3b respectively.

The mini-grain material was uniform and extremely fine with a grain size of ASTM 10 to 12 as shown in Figure 4a. For comparison, the microstructure of standard mini-grain processed material is shown in Figure 4b. An obvious difference between the two mini-grain processed materials was the amount of δ-phase, as shown in Figure 5a and 5b. Recall, that the temperature for the final rotary

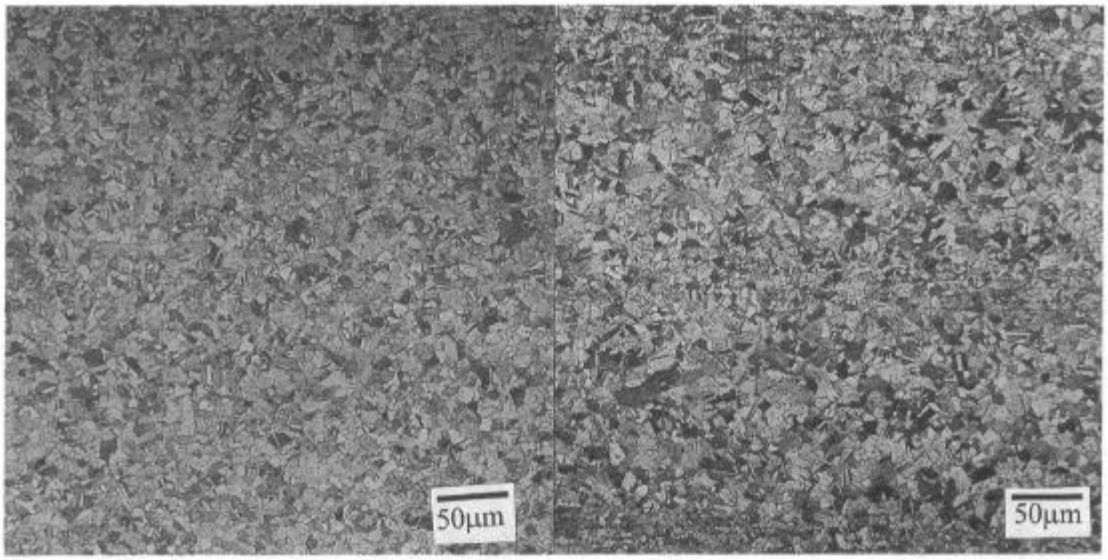

Figure 3a. Microstructure of low C, fine grain processed material. (5-inch diameter)

Figure 3b. Microstructure of standard C, fine grain processed material. (5-inch diameter).

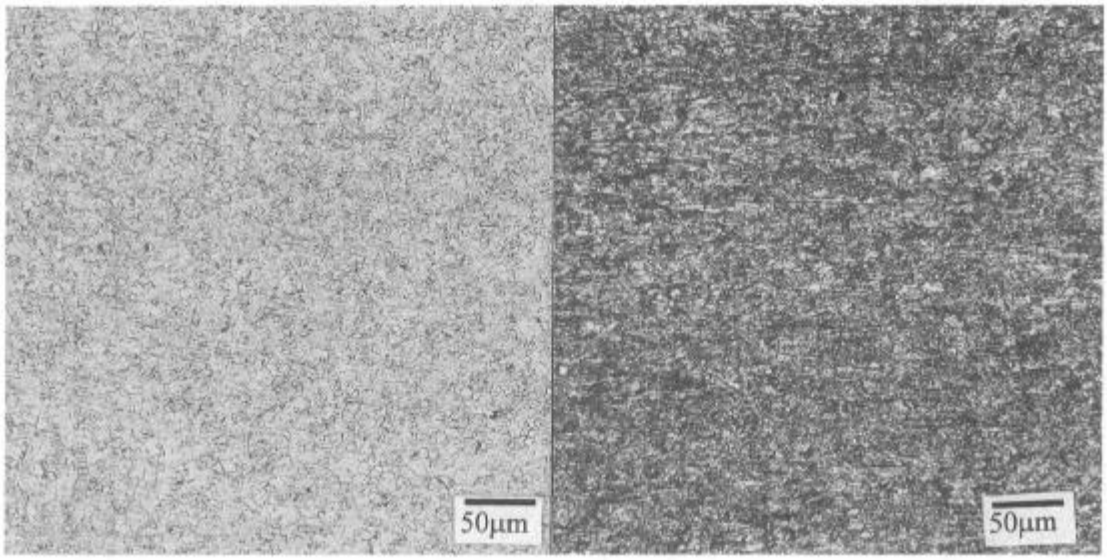

Figure 4a. Microstructure of low C, mini-grain processed material. (5-inch diameter)

Figure 4b. Microstructure of standard mini-grain processed material. (5-inch diameter).

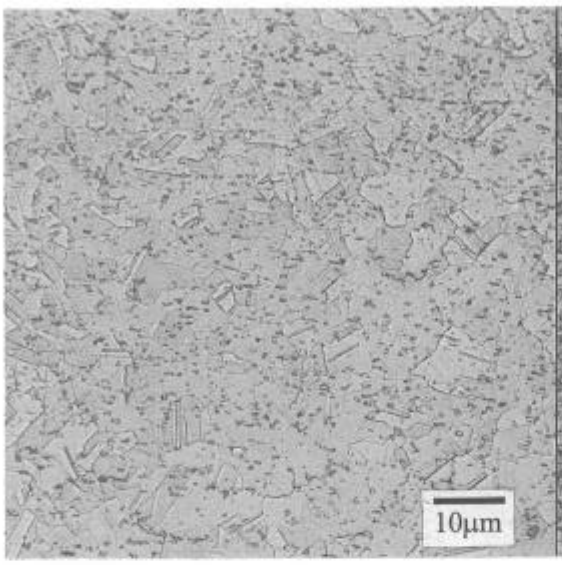

Figure 5a. δ-phase in low C, mini-grain material (5-inch diameter).

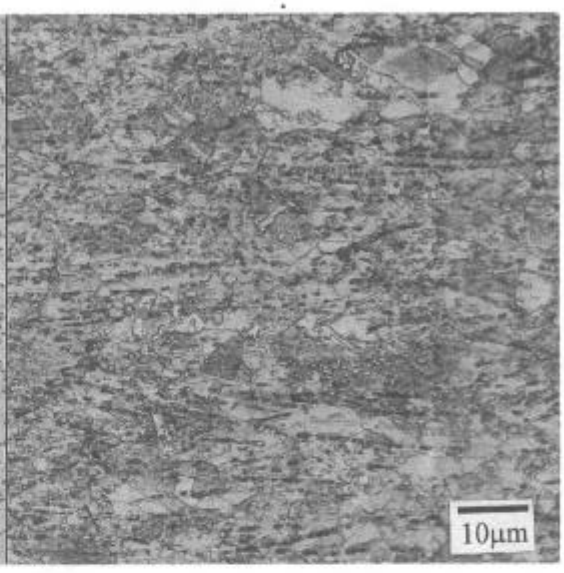

Figure 5b. δ-phase of standard mini-grain material.(5-inch diameter).

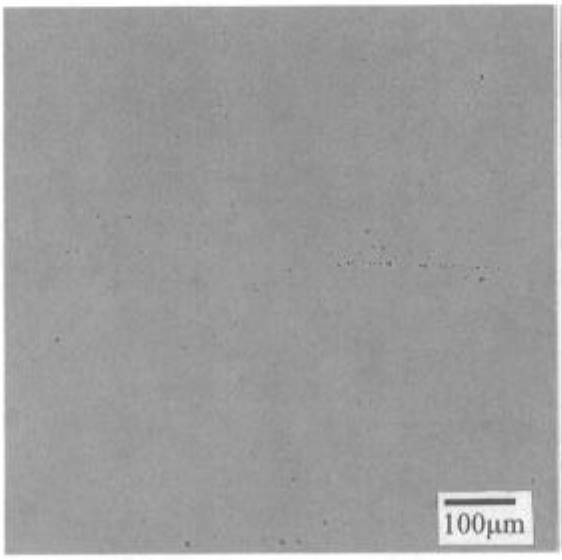

Figure 6a. Typical carbide distribution of 5-inch diameter, low carbon forged bar.

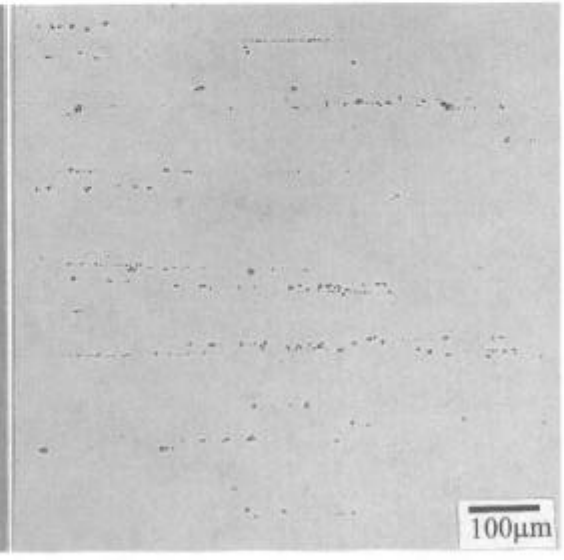

Figure 6b. Typical carbide distribution of 5-inch diameter standard carbon forged bar.

forging was close to the δ-solvus. This facilitated partial solutioning of δ-phase precipitated during the heat treatment and sub-solvus forging. The lower volume of δ-phase in the low carbon mini-grain material resulted in 10 ksi higher yield strength compared to direct aged standard mini-grain material.

Depending on the specific need, this lower δ-phase mini-grain product can benefit forgers since δ-phase precipitated during low temperature forging will also be minimized. Therefore, the solution temperature to achieve high strengths can be slightly lower than for standard mini-grain billet. Improving strength with direct age heat treatments will also be possible with the lower volume fraction of δ-phase.

As expected, the low carbon material exhibited a better carbide distribution than the standard carbon material. As shown in Figure 6a and 6b, the low carbon material contained mostly discrete carbides compared to the standard carbon material which contained numerous stringers.

Tensile Properties - All the material exhibited very high strengths and good ductility that did not vary greatly from one process to another, as shown in Table III through V. The average values for ultimate, yield and ductility are shown in Figure 7a through 7d. The adjustment to Nb made in the low carbon material apparently maintained γ" formation equivalent to the standard chemistry.

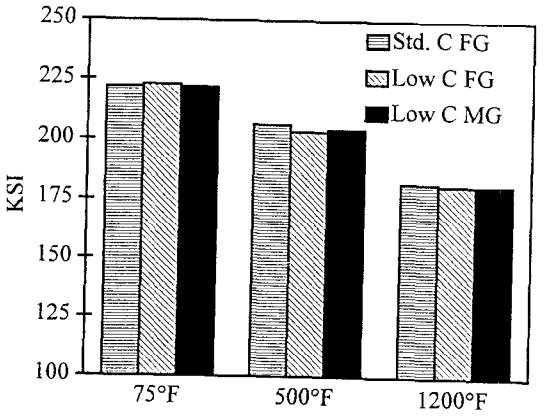

Figure 7a. Average ultimate tensile strengths.

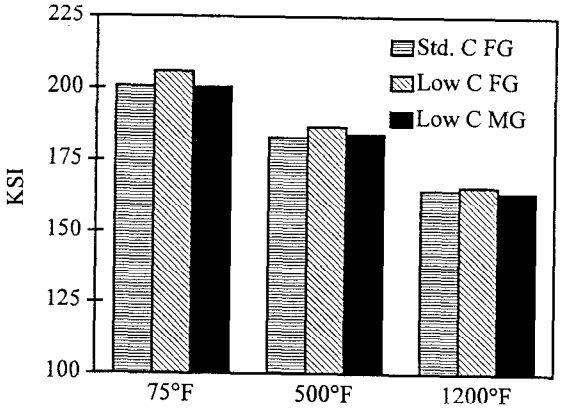

Figure 7b. Average 0.2% offset yield strengths.

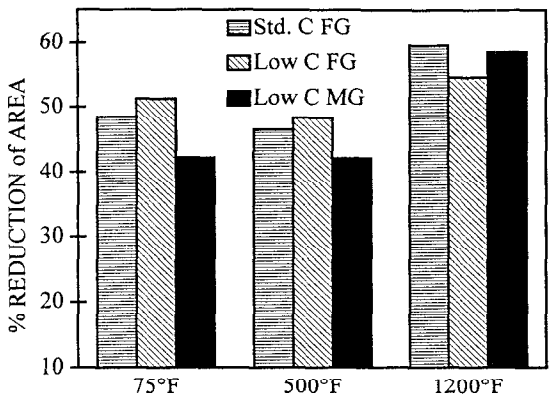

Figure 7c. Average % elongation.

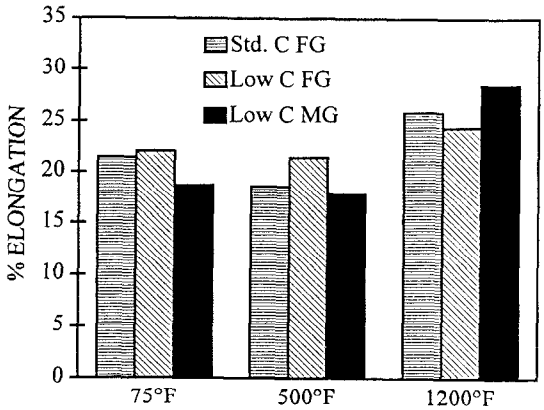

Figure 7d. Average % reduction of area.

Table III. Low Carbon, Fine Grain Tensile Properties.

Position	Test Temperature	UTS (ksi)	0.2% YS (ksi)	%Elong.	%RA
Top	Room	220.2	200.7	25.0	52.3
Top	Room	227.1	213.1	22.6	52.9
Bottom	Room	225.6	212.4	17.3	50.2
Bottom	Room	218.7	197.6	23.2	49.8
	Average	222.9	206.0	22.0	51.3
Top	500°F	203.5	186.9	21.0	49.7
Top	500°F	203.5	186.4	21.8	52.6
Bottom	500°F	204.0	187.3	21.9	45.7
Bottom	500°F	203.4	186.7	20.9	45.2
	Average	203.6	186.8	21.4	48.3
Top	1200°F	180.4	161.9	27.6	54.0
Top	1200°F	184.0	170.1	22.3	53.9
Bottom	1200°F	181.5	168.3	24.2	58.2
Bottom	1200°F	179.8	163.8	23.0	52.2
	Average	181.4	166.0	24.3	54.6

Table IV. Standard Carbon, Fine Grain Tensile Properties.

Position	Test Temperature	UTS (ksi)	0.2% YS (ksi)	%Elong.	%RA
Top	Room	221.8	198.8	21.8	47.5
Top	Room	222.6	205.0	20.5	48.8
Bottom	Room	223.4	201.6	21.7	48.0
Bottom	Room	220.1	197.1	21.5	49.1
	Average	222.0	200.6	21.4	48.4
Top	500°F	207.3	187.2	18.1	48.4
Top	500°F	206.1	181.9	17.7	47.5
Bottom	500°F	205.2	180.2	19.5	44.6
Bottom	500°F	207.0	182.5	18.9	45.4
	Average	206.4	183.0	18.6	46.5
Top	1200°F	183.6	164.1	25.5	59.2
Top	1200°F	180.2	163.0	25.6	58.8
Bottom	1200°F	184.6	167.3	25.7	59.0
Bottom	1200°F	180.0	164.7	26.7	61.5
	Average	182.1	164.8	25.9	59.6

Table V. Low Carbon, Mini-grain Tensile Properties.

Position	Test Temperature	UTS (ksi)	0.2% YS (ksi)	%Elong.	%RA
Top	Room	222.9	202.5	18.3	42.4
Top	Room	221.3	198.1	18.8	40.1
Bottom	Room	222.7	199.3	19.3	41.9
Bottom	Room	221.2	201.2	18.2	44.5
	Average	222.0	200.3	18.7	42.2
Top	500°F	206.3	185.9	16.6	39.7
Top	500°F	202.7	179.3	19.6	41.4
Bottom	500°F	204.8	186.6	16.7	43.0
Bottom	500°F	204.6	184.8	18.8	44.3
	Average	204.6	184.2	17.9	42.1
Top	1200°F	180.7	167.8	27.3	59.7
Top	1200°F	180.9	159.7	27.9	55.8
Bottom	1200°F	184.1	164.9	30.6	60.1
Bottom	1200°F	180.0	163.1	28.2	58.9
	Average	181.4	163.9	28.5	58.6

Creep Properties - The preliminary creep data were consistent with those previously reported by Jackman and Moyer. At this time, two specimens of standard carbon and low carbon, fine grain processed material were tested at each condition. Plots of the average creep strain as a function of time at 1200°F/100 ksi and 1400°F/30 ksi are shown in Figure 8a and 8b, respectively. As shown on the curves, there was very little or no primary creep strain component observed at both test temperatures and the initial creep strain difference at 1200°F and 1400°F was due to elastic strain differences. These preliminary figures indicate no adverse effect in the low carbon material.

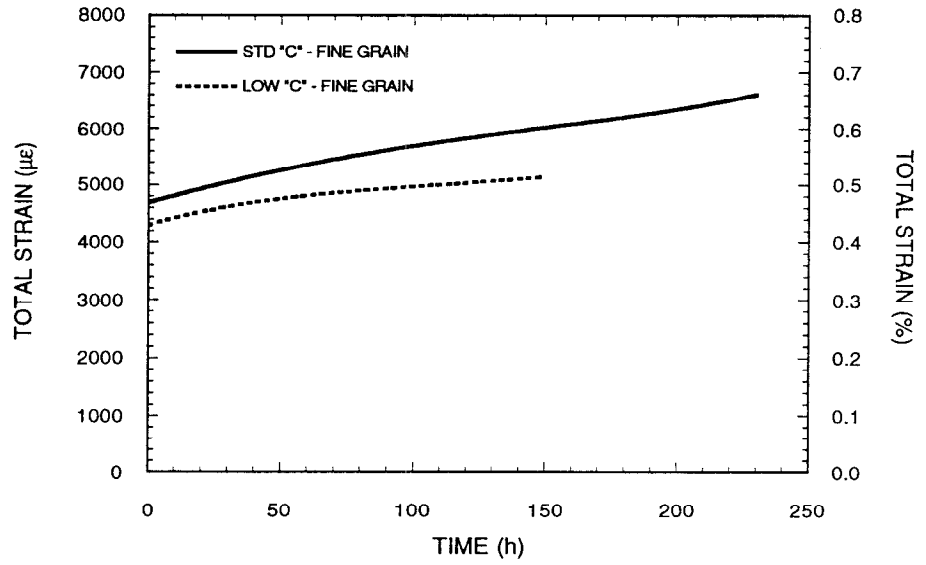

Figure 8a. Average creep strain versus time at 1200°F/100 ksi.

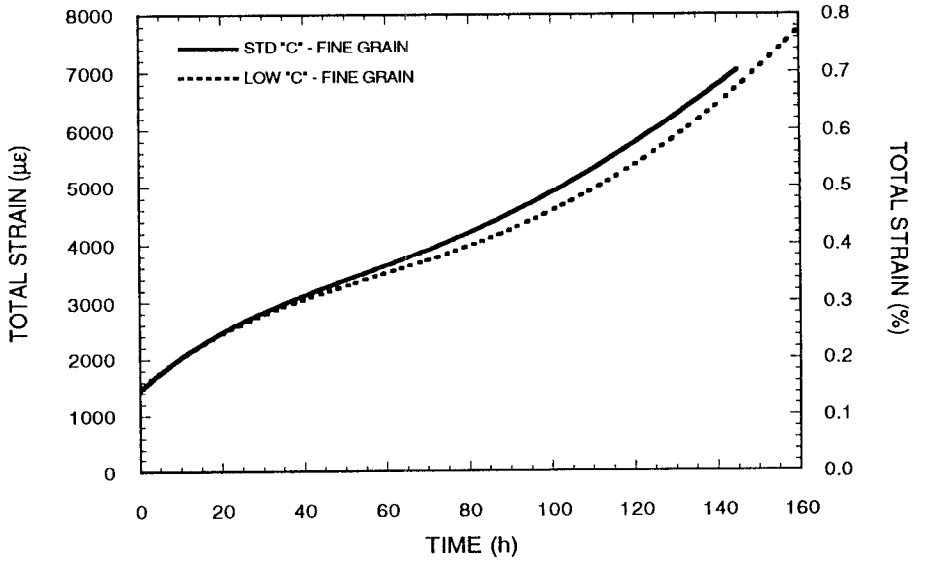

Figure 8b. Average creep strain versus time at 1400°F/30 ksi.

Figures 9a through 9d show the curves of the average creep strain rates overlaid on the creep strain curves for low carbon and standard carbon, fine grain processed material. The curve of creep strain rate was calculated by differentiating the equation for the creep strain versus time.

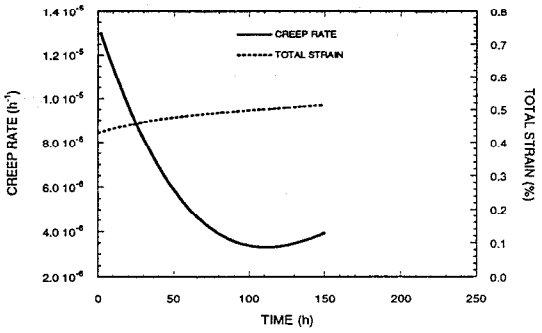

Figure 9a. Average creep strain and creep rate versus time of low C, fine grain material at 1200°F/100 ksi.

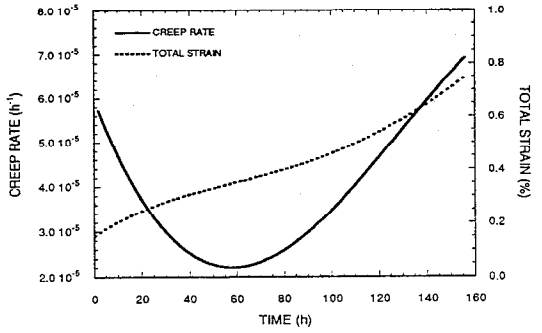

Figure 9b. Average creep strain and creep rate versus time of low C, fine grain material at 1400°F/30 ksi.

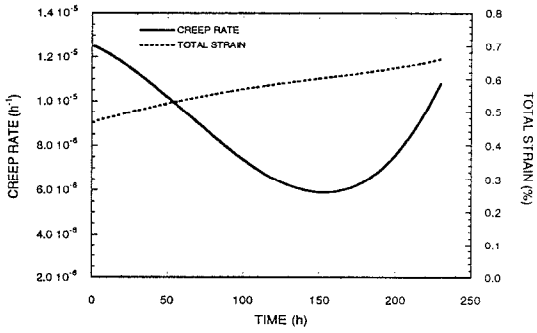

Figure 9c. Average creep strain and creep rate versus time of std. C, fine grain material at 1200°F/100 ksi.

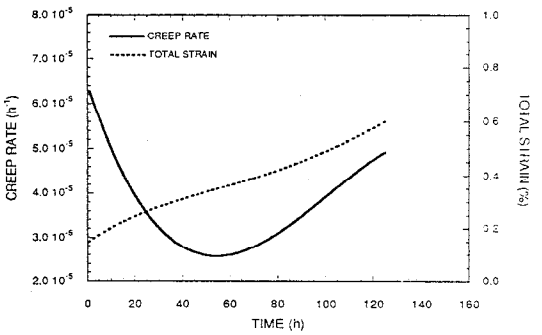

Figure 9d. Average creep strain and creep rate versus time of std. C, fine grain material at 1400°F/30 ksi.

Steady state creep strain and time corresponding to minimum and maximum steady state creep rate for each specimen are listed in Table VI. The steady state creep strains were determined from the first inflection point and minimum point on the creep strain rate curve.[7] There were too few data to draw conclusions at this time, but no major differences were observed between steady state creep of standard carbon and low carbon materials.

Table VI. Minimum and Maximum Steady State Creep Strain of Fine Grain Processed Materials.

Mat'l	Specimen	Temp. (°F)	Stress (ksi)	Elastic Strain (μm)	$\varepsilon_{ss\text{-}min}$ (μm) - Time to $\varepsilon_{ss\text{-}min}$	$\varepsilon_{ss\text{-}max}$ (μm) - Time to $\varepsilon_{ss\text{-}max}$
Low C	91926A1	1200	100	4510	4810 - 17 hrs	6240 - 170 hrs
Low C	91926A3	1200	100	4510	5040 - 20 hrs	5600 - 110 hrs
Low C	91926A4	1400	30	1370	2190 - 11 hrs	4020 - 55 hrs
Low C	91926A5	1400	30	1230	2170 - 19 hrs	2900 - 50 hrs
Std. C	75461A1	1200	100	4180	4740 - 39 hrs	5090 - 120 hrs
Std. C	75641A4	1200	100	4010	4560 - 32 hrs	5080 - 109 hrs
Std. C	75461A2	1400	30	1330	3260 - 35 hrs	3890 - 68 hrs
Std. C	75461A3	1400	30	1280	2040 - 8 hrs	2450 - 28 hrs

Conclusions

1. Low carbon improved the carbide distribution offering the potential for improved low cycle fatigue properties. Low cycle fatigue testing is being performed and data will be available shortly.

2. The preliminary creep data indicated no deleterious effect on creep properties. Creep and stress rupture testing continues. The number of tests being conducted should provide an adequate sample for statistical analysis of the data.

3. The microstructural response to material processing was not effected by lower carbon contents as demonstrated by the fine grain processed material.

4. Tensile strengths were not influenced by carbon content. Low and standard carbon material processed by fine grain techniques exhibited the same tensile properties at the temperatures tested.

5. The mini-grain process used in this program produced material with less matrix δ-phase than the standard mini-grain practice. The lower δ-phase mini-grain process offers certain advantages to forgers.

References

1. J. P. Stroup and L. A. Pugliese, "The Influence of Very Low Carbon Contents on the Properties and Strictures of Nickel-Iron Base Superalloys", paper presented at 96th AIME Annual Meeting, Los Angeles, California, February 1967.

2. J. M. Moyer, "Extra Low Carbon Allvac 718", paper presented at 5th International Symposium on Superalloys, Seven Springs, Pennsylvania, October 1984.

3. L. A. Jackman, M. D. Boldy and A. L. Coffey, "The Influence of Reduced Carbon on Alloy 718", paper presented at 2nd International Symposium on the Metallurgy and Applications of Superalloy 718, 625 and Various Derivatives, Pittsburgh, Pennsylvania, 1991.

4. T. Banik, P. W. Keefe, G. E. Maurer and L. Petzold, "Ultra Fine Grain/Ultra Low Carbon 718", paper presented at 2nd International Symposium on the Metallurgy and Applications of Superalloy 718, 625 and Various Derivatives, Pittsburgh, Pennsylvania, 1991.

5. L. A. Jackman, G. J. Smith, A. W. Dix and M. L. Lasonde, "Rotary Forge Processing of Direct Age Inconel 718 for Aircraft Engine Shafts", paper presented at 2nd International Symposium on the Metallurgy and Applications of Superalloy 718, 625 and Various Derivatives, Pittsburgh, Pennsylvania, 1991.

6. E. E. Brown, R. C. Boettner and D. R. Ruckle, "Minigrain Processing of Ni-based Alloys", 2nd International Symposium on Superalloys, Seven Springs, Pennsylvania, 1972.

7 R. W. Hertzberg, Deformation and Fracture Mechanics of Engineering Materials, John Wiley and Sons, Inc., 1989.

Acknowledgments

The authors would like to acknowledge Jeff Russell (Teledyne Allvac) for his efforts throughout the program, and T. P. Kirkland (HTML) for his help with creep testing.

Part of the research sponsored by the Department of Energy, Assistant Secretary for Energy Efficiency and Renewable Energy, Office of Transportation Technologies, as part of the High Temperature Materials Laboratory User Program, under contract DE-AC05-94OR21400 managed by Martin Marietta Energy Systems, Inc.